Turkish Journal of Electrical Engineering & Computer Sciences

http://journals.tubitak.gov.tr/elektrik/

Research Article

Turk J Elec Eng & Comp Sci
(2017) 25: 4287 – 4298

doi:10.3906/elk-1701-2

Cavitation detection in centrifugal pumps using pressure time-domain features

Pouya SAMANIPOUR, Javad POSHTAN*, Hamed SADEGHI
School of Electrical Engineering, Iran University of Science and Technology, Tehran, Iran

Received: 01.01.2017 • **Accepted/Published Online:** 30.05.2017 • **Final Version:** 05.10.2017

Abstract: Condition monitoring of centrifugal pumps is vital due to their crucial role in industries. One of the most prevalent faults in pumps is cavitation, which can cause mechanical faults or even failure in the pump. In this paper, an approach is suggested to detect cavitation in a centrifugal pump using time-domain analysis of the pressure signal residual. First, pressure and torque signals are obtained using a model of the electro-pump, and then pressure deviation from the pump performance curve is defined as a residual. The residual time-domain features are extracted and applied as inputs to a self-organizing map (SOM) neural network to classify the system modes. The results indicate that the suggested method is capable of detecting incipient cavitation. Furthermore, the suggested method demonstrates robust performance against disturbance.

Key words: Electro-pump, cavitation, fault detection, self-organizing map, time-domain analysis

1. Introduction

Cavitation is one of the most common and destructive faults in centrifugal pumps [1]. Cavitation starts when the pressure in the pumping system reaches a value less than the vapor pressure of the operating point temperature. Vapor bubbles created by the liquid move through the pump. These bubbles turn to liquid unexpectedly at a place with higher pressure, and it occurs as a collapse. The cavitation leads to erosion or shock in pumping proportional to fault intensity. Hence, cavitation detection is one of the most frequently discussed topics due to its harmful effects [2–6].

Signal-based approaches are among the common approaches in cavitation detection. In these approaches, different signals such as vibration, pressure, acoustic emission, and electrical currents are utilized to detect a possible fault in the centrifugal pumps. Frequency-domain analysis is the most common method to detect potential faults. Each fault has a specific signature in the spectrum of the signals. Therefore, the signature analysis in the frequency domain would provide valuable information to determine the health status of the system. Moreover, time-domain analysis is discussed in the literature, and in this method the trend of the signals can provide a vital insight into health status.

Vibration analysis is the most prevailing approach exploited to detect faults in centrifugal pumps [7]. Wang and Chen presented an intelligent diagnosis method based on features of the vibration signal. In this method, a wavelet was employed to extract features from vibration signals, and the rough set was utilized to provide diagnosis knowledge for a neural network [8]. Sakthivel et al. utilized a decision tree to extract statistical features from vibration measurement and classify these features simultaneously. Outcomes indicated that this method can detect various faults in a monoblock pump with high precision [9]. Muralidharan and Sugurmaran

*Correspondence: jposhtan@iust.ac.ir

utilized a discrete wavelet transform to extract features from vibration signals, and rough sets to generate rules. Then a fuzzy system was employed to classify the features based on extracted rules, and the outcomes indicated 99% accuracy in classification [10]. Sakthivel et al. extracted statistical features from vibration signals; then they constituted a set with extracted features. The dimension of the feature set was reduced using various techniques and then the reduced set was applied to a decision tree to classify different modes of the pump [11]. McKee et al. suggested a new method for detecting cavitation based on spectral and statistical methods. In this method, octave band analysis, principal component analysis, and statistical metrics are employed to detect cavitation from vibration signals, and then Mahalanobis distance is utilized to set thresholds. This method is tested on various types of industrial pumps [12]. One of the main challenges in detecting cavitation based on vibration analysis is the cost of sensors. In addition, identifying the relation between faults and signature in the spectrum of the signal would be crucial due to the complexity of industrial systems.

Acoustic emission has recently been discussed as a superior tool to detect faults in centrifugal pumps. Alfayez et al. utilized acoustic emission to detect cavitation by showing that the cavitation decreases acoustic emission level. This method also determines the best efficiency point of the centrifugal pump [13]. Farokhzad et al. employed a multilayer perceptron neural network to classify features extracted from acoustic signals. The results demonstrated 98% precision in detecting cavitation [14]. The main challenge to detect faults with acoustic emission is the high cost of the related sensors.

Hence, electrical current sensors were introduced as an alternative to vibration and acoustic signals, for these are already available in most industrial systems. Therefore, implementation cost is reduced by using these signals. Durocher et al. utilized stator current sidebands to detect cavitation; sidebands amplitudes are increased because of cavitation occurrence. A threshold was utilized to detect cavitation [15]. Hernandez-Solis et al. employed motor current signals and a power spectrum to detect cavitation. The correlation between cavitation and the power spectrum was discussed in different operation points [16]. The main challenge in using motor current signals is that the induction motor is a low pass filter; therefore, fault components in high frequencies are eliminated.

Therefore, Stopa et al. proposed a novel method to detect cavitation using torque. In this approach, a nonlinear model for an induction motor was extracted. Then the torque was estimated based on the model, and the spectrum of the estimated torque was employed to detect cavitation. The results showed that there was a strong correlation between cavitation and sidebands of the torque signal [17]. Though using the incremental encoder to estimate torque would be crucial, this method was introduced as an alternative to motor current signature analysis.

In this paper, to overcome these difficulties an approach is suggested for detecting cavitation in pumps at early stages. First, a nonlinear model of the electro-pump is extracted. Pump pressure and torque are obtained using the nonlinear model of the electro-pump and pump characteristics curves. It is proven that cavitation leads to deviations from these curves. Therefore, the deviation of the pump pressure from the curve is defined as a residual. Time-domain features are extracted from this residual and apply to a self-organizing map (SOM) neural network, and the network outputs are modes of the pump, healthy and cavitation. The results show that this method is capable of detecting cavitation at early stages with high precision. The supremacy of this method is as follows: first, this method does not require vibration and acoustic measurements, and it could be implemented by electrical currents, voltages sensors, and pressure sensors; hence, the implementation cost would be reduced. Moreover, this method is robust to disturbances, which can have considerable effects on the results of a fault diagnosis system. Disturbances in centrifugal pumps vary pressure, flow, and torque values,

though these variations are based on pump characteristics curves. Therefore, disturbances would not lead to a false alarm with respect to the defined residual that determines deviations from pump curves.

2. Electro-pump's dynamic model

In this section, a nonlinear model of an electro-pump is presented. A block diagram of the motor-pump set is shown in Figure 1 [18]. The dynamic model of an electro-pump can be expressed as follows [19,20]:

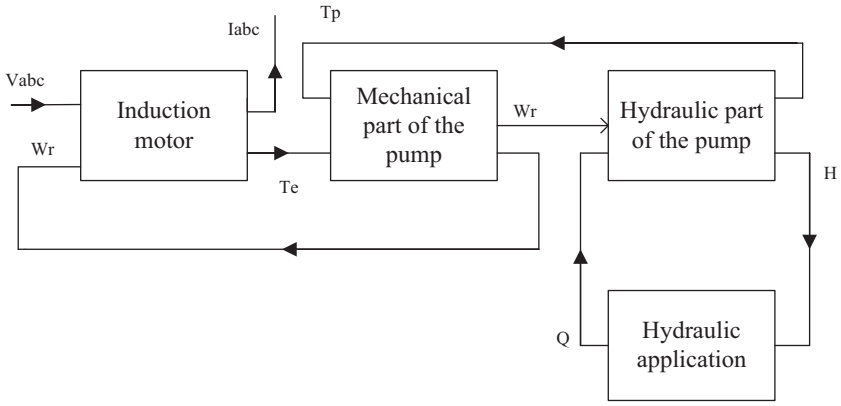

Figure 1. Electro pump structure.

$$\dot{x}=f\left(x\right)+Gu+m\left(x,Q\right) \tag{1}$$

In this equation, state variables are as follows:

$$x=[\psi_{qs}\,\psi_{ds}\,\psi_{qr}\,\psi_{dr}\,\omega_r]^T \tag{2}$$

The input vector can be expressed as follows:

$$u=[\,v_{sq}\quad v_{sd}]^T \tag{3}$$

$f\left(x\right)$, G and m can be expressed as follows:

$$f\left(x\right)=\begin{pmatrix} \omega_b\left[-\frac{r_s(X_{lr}+X_M)}{D}\psi_{qs}-\frac{\omega}{\omega_b}\psi_{ds}+\frac{r_sX_M}{D}\psi'_{qr}\right] \\ \omega_b\left[\frac{\omega}{\omega_b}\psi_{qs}-\frac{r_s(X_{lr}+X_M)}{D}\psi_{ds}+\frac{r_sX_M}{D}\psi'_{dr}\right] \\ \omega_b\left[\frac{r_sX_M}{D}\psi_{qs}-\frac{r_s(X_{ls}+X_M)}{D}\psi'_{qr}-\frac{\omega-\omega_r}{\omega_b}\psi'_{dr}\right] \\ \omega_b\left[\frac{r_sX_M}{D}\psi_{ds}+\frac{\omega-\omega_r}{\omega_b}\psi'_{qr}-\frac{r_s(X_{ls}+X_M)}{D}\psi'_{dr}\right] \\ \frac{T_e}{J}-\frac{B\omega_r}{J} \end{pmatrix} \tag{4}$$

$$G=\begin{pmatrix} \omega_b & 0 \\ 0 & \omega_b \\ 0 & 0 \\ 0 & 0 \\ 0 & 0 \end{pmatrix}, m(x,Q)=\begin{pmatrix} 0 \\ 0 \\ 0 \\ 0 \\ \frac{-1}{j} f_T(Q,\omega_r) \end{pmatrix} \tag{5}$$

In Eq. (4), D is defined as follows:

$$D=X_{ls}X_{lr}+X_{ls}X_M+X_{lr}X_M \tag{6}$$

The variables and parameters in Eqs. (1) to (5) are introduced in Table 1.

In Eq. (5), f_T represents the torque produced by the hydraulic part of the pump. The hydraulic part

Table 1. The electro-pump variables and parameters and their description.

Variables and parameters	Description
$(\quad)_{s(r)}$	Stator (rotor) circuits
p	Derivative operation
ψ_{dq0}	Flux linkage in $dq0$ frame
R	Resistance
X_m	Magnetizing reactance
X_l	Leakage reactance
V_{dq0}	Power supply voltage in $dq0$ frame
I_{dq0}	Stator currents in $dq0$ frame
ω	Rotating circuits angular velocity
ω_r	Angular velocity of the induction motor
ω_b	Base electrical rotating velocity
T_e	Electromagnetic torque
T_p	Pump torque
Q	Fluid flow
H	Pressure
$a_{ti}(a_{hi})$	Parameters of the hydraulic part of the pump
B	Friction coefficient
J	Inertial coefficient
P	Number of poles
K_i	Fault intensity multipliers
f_c	Fault occurrence multiplier
h	Delivery head of the pump
h_{rr}	Pipe resistant coefficient

can be expressed by torque, and pressure difference between outlet and inlet of the pump, and these variables can be obtained as follows [20]:

$$f_H = H{=}\rho g\left(-a_{h2}Q^2{+}a_{h1}\omega_r Q{+}a_{h0}\omega_r^2\right) \tag{7}$$

$$f_t = T_p{=}-a_{t2}Q^2{+}a_{t1}\omega_r Q{+}a_{t0}\omega_r^2 \tag{8}$$

The parameters and variables in Eqs. (7) and (8) are introduced in Table 1.

In this paper, the hydraulic application is considered as a closed-loop pipe circuit and the delivery head can be obtained as follows [21]:

$$h{=}h_{rr}Q^2 \tag{9}$$

A schematic diagram of the electro-pump is depicted in Figure 2.

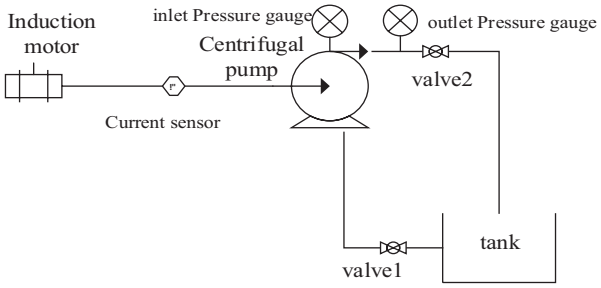

Figure 2. A schematic diagram of the electro-pump.

2.1. Cavitation model

As mentioned earlier, cavitation can cause mechanical failure in the pump. In this paper, the hydraulic behavior of the pump is considered in order to detect cavitation, and this performance is determined by the pump parameters, which can be changed within cavitation occurrence. Therefore, cavitation occurrence leads to variation in the hydraulic performance of the pump, and it decreases the level of fluid flow and pressure, and also it deteriorates pump efficiency. A linear approximation of cavitation impact on the hydraulic performance of the pump can be expressed as follows [20]:

$$H{=}\rho g\left(-a_{h2}Q^2{+}a_{h1}\omega_r Q{+}a_{h0}\omega_r^2\right){-}k_1 f_c \tag{10}$$

$$T_p{=}-a_{t2}Q^2{+}a_{t1}\omega_r Q{+}a_{t0}\omega_r^2{-}k_2 f_c \tag{11}$$

As can be observed in Eqs. (10) and (11) cavitation can change the pump characteristic curves, and as mentioned earlier it decreases the pump pressure and torque simultaneously.

The precise model of the cavitation in a pump would be nonlinear and complex. The model used in this paper is linear, which approximately demonstrates the impact of cavitation on the performance of the hydraulic part of the pump. The main point is that cavitation occurrence based on a complex nonlinear model in a laboratory system would deviate the residual from zero, and this deviation is the subject of this study.

3. Fault detection algorithm

With respect to Eqs. (10) and (11), cavitation will be reflected in the hydraulic behavior of the pump, and it can change torque and pressure values. The main effect of the hydraulic faults is that the value of the torque and pressure, which are produced by the impeller, will change. There are a number of factors that can cause bubble formation in the pump such as upstream compressibility and flow reversal. Given that, the experimental setup utilized in this paper has a closed-loop piping system as can be observed in Figure 2. Therefore, flow reversal and upstream compressibility could not affect the pump. In addition, the presence of only one valve in the outlet of the pump mitigates the water hammer and nonfully developed flow. Therefore, we interpret that these effects are insignificant for the purpose of the current study. Moreover, external factors such as disturbance may also affect the pressure and torque values. On the other hand, the main effect of the mechanical fault such as wear of bearing, wear of seal, and rub-impact between the impeller and the casing is vibration and leakage in the pump [18]. Hence, a residual signal is defined as the following in order to avoid false alarms due to disturbances:

$$r_1 = H - \rho g(-a_{h2}Q^2 + a_{h1}\omega_r Q + a_{h0}\omega_r^2) \tag{12}$$

In this equation, deviation of the pump pressure measurement values from the pump curve is considered as the residual. Therefore, with respect to the fact that disturbance cannot change pump curves, the residual would be robust against disturbances. However, the residual is obtained using measurement values of pressure, fluid flow, and angular speed. In order to avoid using supplementary sensors, a number of equations will be presented to obtain angular speed and fluid flow.

Angular speed can be obtained using a state observer, which is discussed in [22], and the equation is as follows:

$$\hat{\omega}_r = K_P\left(e_{ids}\hat{\psi}_{qr} - e_{iqs}\hat{\psi}_{dr}\right) + K_I\int(e_{ids}\hat{\psi}_{qr} - e_{iqs}\hat{\psi}_{dr})dt \tag{13}$$

In this equation, e_{ids} and e_{iqs} represent the current estimation errors, while $\hat{\psi}_{qr}$ and $\hat{\psi}_{dr}$ represent the estimated flux linkage in the dq frame. K_i and K_p represent the regulation coefficients [22].

Furthermore, the fluid flow can be acquired by using Eq. (8) as follows:

$$Q = \frac{a_{t1}\omega_r + \sqrt{a_{t1}^2\omega_r^2 - 4a_{t2}(T_P - a_{t0}\omega_r)}}{2a_{t2}} \tag{14}$$

In this equation, the pump torque in the steady-state mode ($\frac{d\omega_r}{dt} \approx 0$) can be obtained by the following equation:

$$\hat{T}_P = \hat{T}_e - B\hat{\omega}_r \tag{15}$$

In Eq. (15), the electromagnetic torque can be obtained as follows [22]:

$$\hat{T}_e = \frac{P}{2}\frac{1}{\omega_b}\left(\hat{\psi}_{ds}\hat{i}_{qs} - \hat{\psi}_{qs}\hat{i}_{ds}\right) \tag{16}$$

Consequently, the unknown variables such as angular speed and fluid flow in the residual equation are obtained using Eqs. (13) and (14). Therefore, the residual can be obtained using electrical sensors and a pressure sensor.

As mentioned earlier, variations in the residual can provide useful information about the pump health status. Therefore, a number of static features are extracted from the residual and applied to the classification algorithm. These features are presented as follows:

1. Minimum and maximum values: it refers to minimum and maximum of the residual.
2. Variance: it is the variance of the signal and the formula is as follows:

$$variance = \frac{\sum (x-\bar{x}_i)^2}{n(n-1)} \tag{17}$$

In this equation, $\bar{x}_i$ is the mean value of the signal and n is the number of samples.

3. The final feature is the mean value of the residual signal.

In order to classify these features a classification algorithm is required, and in this paper self-organizing map (SOM) is employed to classify the pump modes. SOM is an effective tool to cluster the data and is presented by Kohonen [23]. It is an unsupervised neural network that attempts to represent the input data in a low-dimensional grid [24]. The main important three phases of SOM designing can be expressed as follows [25]:

1. Competition phase: $x \epsilon R^n$ is chosen randomly from the input space. Euclidean distance of x to each cluster center (w_j) is calculated. The shortest distance determines the winner neuron. The competitive phase can be expressed as follows:

$$i(x) = arg \|x-w_j\| \tag{18}$$

In Eq. (18), w_j represents the cluster weights, where $j = 1, 2, \ldots, m$ $(m < n)$ and $i(x)$ represents the winner neuron index.

2. Cooperative phase: the winner neuron tends to excite the other neuron. The neighborhood function can be expressed as follows:

$$h_{ij}(x,t) = \exp(-\frac{d_{ij}^2}{2\delta(t)^2}) \tag{19}$$

In this equation d_{ij} is the lateral distance between the winning neuron and the excited neuron j, δ is the effective width, and t is the number of iterations. δ is chosen as a Gaussian function; thus the effective width decreases with the iteration increase as the following:

$$\delta(t) = \delta_0(\exp(-\frac{t}{\tau})) \tag{20}$$

In Eq. (20), δ_0 and τ represent the initial effective width and the time constant, respectively. It can be observed in Eq. (19) that the network convergence rate is high at early iterations.

3. Adaptive phase: in this phase, initial weights are updated as follows:

$$w_j(t+1) = w_j(t) + \eta(t) h_{ij}(xt)(x-w_j(t)) \tag{21}$$

In Eq. (21), η represents the learning rate defined as a Gaussian function as follows:

$$\eta(t) = \eta_0 \exp(-\frac{t}{\tau_0}) \tag{22}$$

In Eq. (22), η_0 represents the initial learning rate, and it is chosen between zero and one, and τ_0 represents the learning rate time constant.

4. Continue with phase 1 until no noticeable changes in the weight updating are seen.

The neural network structure is shown in Figure 3.

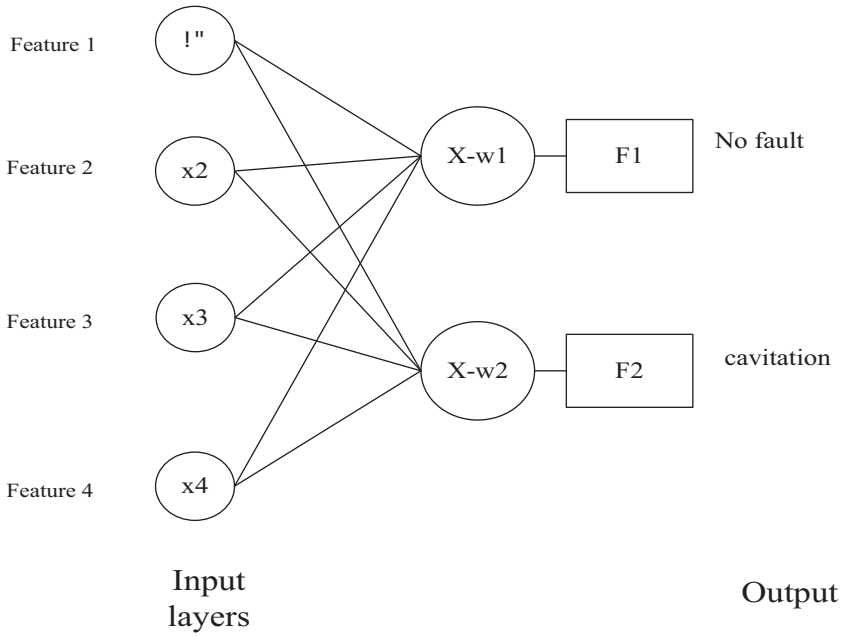

Figure 3. Neural network structure.

4. Simulation results

In this section, an electro-pump is simulated by Eqs. (1) to (5). The induction motor is a 3-kW, 3000-rpm, 220-V, 50-Hz squirrel-cage motor. The induction motor parameters shown in Table 2 are extracted from a laboratory system. The pump parameters shown in Table 3 belong to a 3-stage centrifugal pump [26]. The electro-pump model expressed by Eqs. (1) to (5) is simulated by using the presented parameters, and the results demonstrate that this model has high precision in steady state [26]. Moreover, cavitation is modeled on the dynamic model according to Eqs. (10) and (11). The pressure and torque signals with and without cavitation are depicted in Figures 4 and 5. As can be observed cavitation is applied to the model at $t = 3$ in steady state, and cavitation leads to variations in the pressure and torque signals of the pump.

Table 2. Induction motor parameters.

Induction motor parameters	r_s	r_r	X_{ls}	X_{lr}	X_M	J
Parameters value	1.64	1.9	3	3	78.57	0.089

Table 3. Centrifugal pump parameters.

	a_0	a_1	a_2
H_p	0.0631	652.9630	0.683e+07
T_p	–0.001	974.8148	–1.403e+07

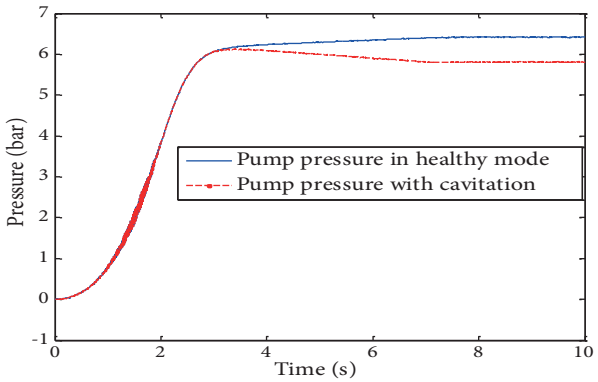

Figure 4. Simulated pump pressure with and without fault.

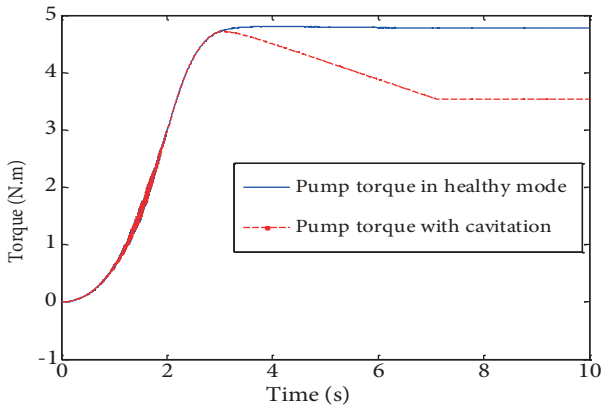

Figure 5. Simulated pump torque with and without fault.

One of the main properties of the suggested method is robustness to disturbance. The disturbance is applied to fluid flow in order to evaluate the robustness of the algorithm as follows:

$$Q_{new}=Q+d \tag{23}$$

In Eq. (23) d is the disturbance applied to fluid flow, which can lead to variations in the fluid flow of the pump. Consequently, these variations lead to changes in the torque and pressure of the pump according to Eqs. (7) and (8). Disturbance is defined as a pulse as can be observed in Figure 6, and applied to the pump at $t = 3$. In normal mode, an increase in the flow leads to a decrease in the pressure, and also an increase in the torque according to pump characteristic curves. However, at the time of cavitation torque, pressure and flow do not behave according to pump characteristics curves: they all decrease simultaneously. In Figure 7 the impact of the disturbance on the residual is shown in both healthy and faulty modes. As can be observed, in the healthy mode the disturbance does not deviate the residual in steady state, and also it will not lead to false alarms. In Figure 7, residual variations in the first instants are due to observation errors of the angular velocity. The observer in Eq. (13) has errors in the transient mode, although in the steady state the observation error will converge to zero; therefore as can be observed the residual will remain close to zero in steady state. Other variations in the residual signal are due to measurement noise applied to the system. Therefore, the proposed algorithm is capable of showing robust performance against disturbances. Furthermore, in Figure 7 the residual is shown at the time of cavitation in the presence of the disturbance. Cavitation is applied to the pump according to Eqs. (10) and (11), and it is applied gradually due to the way that cavitation occurs in industrial systems. Cavitation gradually decreases pump pressure as well as fluid flow, and it deteriorates pump efficiency. As can be observed in Figure 7 cavitation leads to gradual variations in the residual signal and the residual reaches a constant value eventually. In this paper, 10% and 20% variations in the pressure are considered as the maximum variation caused by cavitation. The deviation caused by cavitation is the source of information to detect cavitation. Therefore, time-domain features as mentioned earlier are extracted from the residual signal to detect cavitation in the centrifugal pump. These features are extracted in the steady state in the presence of the disturbance, and in the following form:

- 75 samples are extracted in the normal mode using Eqs. (7) to (10) with the measurement noise.
- 75 samples are extracted in type-1 cavitation mode. In this mode k_1 and k_2 in Eqs. (10) and (11) are defined in a way such that torque and pressure variations are 5% to 10%.

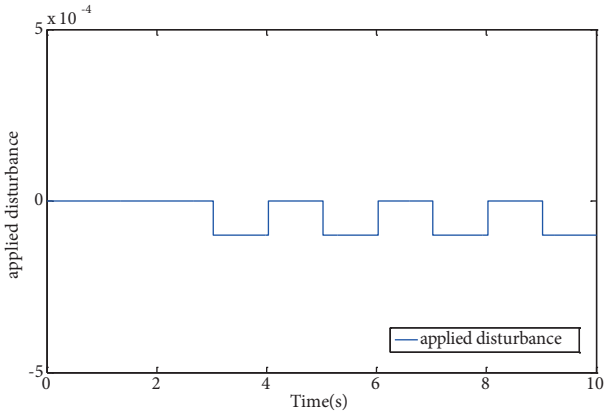

Figure 6. Applied disturbance on the fluid flow at

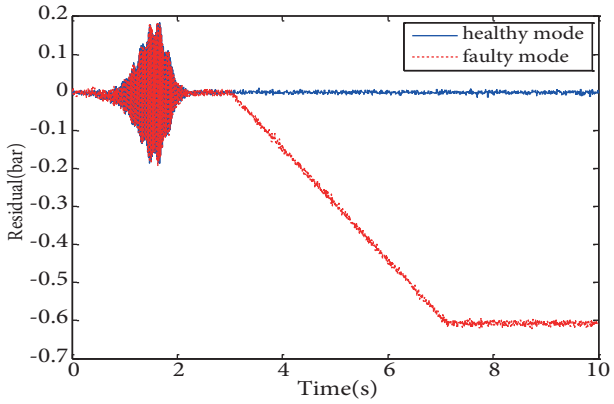

Figure 7. The residual in the presence of the disturbance.

- 75 samples are extracted in type-2 cavitation mode. In this mode k_1 and k_2 multipliers in Eqs. (10) and (11) are defined in a way such that torque and pressure variations are 10% to 20%.

Extracted features of the residual in type-1 cavitation can be seen in Figure 8. As can be observed, the features are deviated from zero. With respect to the way that the residual is defined the minimum values and the mean values are negative. The minimum value of the signal is the most distinctive feature because it has the greatest amount of deviation from zero as can be observed in Figure 8.

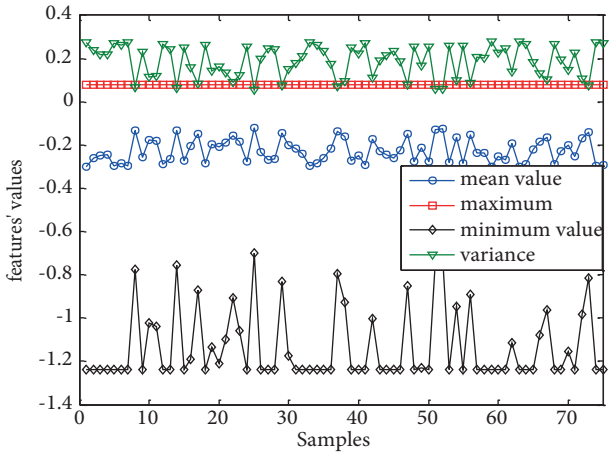

Figure 8. Extracted features of the residual with type-1 cavitation.

The features in the normal mode and both cavitation modes are utilized as the inputs of the SOM to train the network; 150 random samples composed of 50 samples in normal mode, 50 samples of type-1 cavitation, and 50 samples of type-2 cavitation are exploited for training, and 75 samples are utilized to test it. The SOM utilized these features to classify 3 modes of the pump and the test results are presented in Table 4.

As can be observed, the SOM can detect the healthy mode of the pump with high precision. Moreover, in type-1 cavitation 23 test samples are detected correctly with respect to the fact that variations in the pressure are less than 10%. At the time of type-2 cavitation, with respect to the fact that pressure variations are between 10% and 20%, the SOM can detect 24 test samples correctly. The results show that the accuracy in the detection of the type-1 cavitation is 88%, and when type-2 cavitation occurs the algorithm shows better precision with an

Table 4. SOM results within cavitation.

	Training data	Test samples	Number of detection	Accuracy of the classification
Normal mode	50	25	24	96%
Type-1 cavitation	50	25	22	88%
Type-2 cavitation	50	25	24	96%

accuracy above 96%. In type-2 cavitation the residual is more deviated from zero. Therefore, the time-domain features would be more distinctive rather than in the healthy mode, and it would be easier for the SOM to classify these modes.

5. Conclusion

In this paper, a simple structure high-precision method is presented to detect cavitation in an electro-pump. In this method, a residual is defined, and the most significant feature of the residual is robustness against disturbances. In addition, this method does not require vibration and acoustic sensors and it can be implemented with electrical sensors and a pressure sensor; therefore, implementation cost will be reduced.

In this paper, a nonlinear model that describes the healthy status of the electro-pump is presented; also the impact of the cavitation on the hydraulic part of the pump is discussed and modeled. With respect to the cavitation impact on the behavior of the system, a residual that is robust against disturbances is defined. This residual shows deviations of the pump behavior from the pump curves; therefore, the disturbance cannot lead to the deviation, for variations that are caused by disturbance would behave based on pump curves. Then time-domain features are extracted from the residual and applied to a classification algorithm, which is SOM in this paper. The SOM classifies modes of the pump as healthy and cavitation. The results show that this method is capable of detecting cavitation with 88% precision. The precision of the presented method is lower than that of methods that use vibration and acoustic sensors; on the other hand, this method has the advantage of disturbance rejection as well as low implementation cost. Furthermore, the effectiveness of the classification algorithm can be improved by using an optimization method in order to choose initial weights of the SOM algorithm, and it will be considered in future works.

References

[1] McKee KK, Forbes G, Mazhar I, Entwistle R, Howard I. A review of major centrifugal pump failure modes with application to the water supply and sewerage industries. In: ICOMS Asset Management Conference; 2011. pp. 32.

[2] Al-Hashmi S, Gu F, Li Y, Ball AD, Fen T, Lui K. Cavitation detection of a centrifugal pump using instantaneous angular speed. In: ASME 7th Biennial Conference on Engineering Systems Design and Analysis. American Society of Mechanical Engineers; 2004. pp. 185-190.

[3] Dalton T, Patton R. Model-based fault diagnosis of a two-pump system. T I Meas Control 1998; 20: 115-124.

[4] McKee KK, Forbes GL, Mazhar I, Entwistle R, Howard I. A review of machinery diagnostics and prognostics implemented on a centrifugal pump. In: Engineering Asset Management 2011. Springer; 2014. pp. 593-614.

[5] Parrondo JL, Velarde S, Santolaria C. Development of a predictive maintenance system for a centrifugal pump. JQME 1998; 4: 198-211.

[6] Jensen J. Detecting Cavitation in Centrifugal Pumps Experimental Results of the Pump Laboratory. ORBIT second quarter 2000; 26-30.

[7] Peck JP, Burrows J. On-line condition monitoring of rotating equipment using neural networks. ISA T 1994; 33: 159-164.

[8] Wang H, Chen P. Intelligent diagnosis method for a centrifugal pump using features of vibration signals. Neural Comput Appl 2009; 18: 397-405.

[9] Sakthivel NR, Sugumaran V, Babudevasenapati S. Vibration based fault diagnosis of monoblock centrifugal pump using decision tree. Expert Syst Appl 2010; 37: 4040-4049.

[10] Muralidharan V, Sugumaran V. Rough set based rule learning and fuzzy classification of wavelet features for fault diagnosis of monoblock centrifugal pump. Measurement 2013; 46: 3057-3063.

[11] Sakthivel NR, Nair BB, Elangovan M, Sugumaran V, Saravanmurugan S. Comparison of dimensionality reduction techniques for the fault diagnosis of mono block centrifugal pump using vibration signals. Engineering Science and Technology, an International Journal 2014; 17: 30-38.

[12] McKee KK, Forbes G, Mazhar I, Entwistle R, Hodkiewicz M, Howard I. A single cavitation indicator based on statistical parameters for a centrifugal pump. In: Proceedings of the 7th World Congress on Engineering Asset Management (WCEAM 2012). Springer; 2015. pp. 473-481.

[13] Alfayez L, Mba D, Dyson G. The application of acoustic emission for detecting incipient cavitation and the best efficiency point of a 60kW centrifugal pump: case study. NDT E Int 2005; 38: 354-358.

[14] Farokhzad S, Ahmadi H. Acoustic Based Cavitation Detection of Centrifugal Pump by Neural Network. Journal of Mechanical Engineering and Technology 2013; DOI: 10.18005/JMET0101001.

[15] Durocher DB, Feldmeier GR. Predictive versus preventive maintenance. IEEE Ind Appl Mag 2004; 10: 12-21.

[16] Hernandez-Solis A, Carlsson F. Diagnosis of submersible centrifugal pumps: a motor current and power signature approaches. EPE J 2010; 20: 58-64.

[17] Stopa MM, Filho BJC, Martinez CB. Incipient detection of cavitation phenomenon in centrifugal pumps. IEEE T Ind Appl 2014; 50: 120-126.

[18] Kallesoe CS. Fault detection and isolation in centrifugal pumps. PhD, Alborg University, Alborg, Denmark, 2005.

[19] Krause PC, Wasynczuk O, Sudhoff SD, Pekarek S. Analysis of Electric Machinery and Drive Systems. New York, NY, USA: John Wiley & Sons, 2013.

[20] Kallesøe CS, Cocquempot V, Izadi-Zamanabadi R. Model based fault detection in a centrifugal pump application. IEEE T Contr Syst T 2006; 14: 204-215.

[21] Isermann R. Fault-diagnosis applications: model-based condition monitoring: actuators, drives, machinery, plants, sensors, and fault-tolerant systems. Berlin, Germany: Springer Science & Business Media, 2011.

[22] Kubota H, Matsuse K, Nakano T. DSP-based speed adaptive flux observer of induction motor. IEEE T Ind Appl 1993; 2: 344-348.

[23] Kohonen T. The self-organizing map. In: Proc IEEE 78; September 1990. pp. 1464-1480.

[24] Mingoti SA, Lima JO. Comparing SOM neural network with fuzzy c-means, K-means and traditional hierarchical clustering algorithms. Eur J Oper Res 2006; 174: 1742-1759.

[25] Haykin S. Network Networks. A Comprehensive Foundation. Upper Saddle River, NJ, USA: Prentice Hall, 2004.

[26] Samanipour P, Poshtan J. Electro Pump Modeling Using Laboratory System Data. In: Power Electronics and Drive Systems Technologies Conference (PEDSTC). IEEE; 2016. pp. 111-115.